

GPS precise tracking of TOPEX/POSEIDON: Results and implications

W. I. Bertiger, Y. E. Bar-Sever, E. J. Christensen, E. S. Davis, J. R. Guinn, B. J. Haines,
R. W. Ibanez-Meier, J. R. Jee, S. M. Lichten, W. G. Melbourne, R. J. Muellerschoen,
T. N. Munson, Y. Vigue, S. C. Wu, and T. P. Yunck

Jet Propulsion Laboratory, California Institute of Technology, Pasadena

B. E. Schutz, P. A. M. Abusali, H. J. Rim, M. M. Watkins

Center for Space Research, University of Texas at Austin

P. Willis

Institute Géographique National, France

Abstract. A reduced dynamic filtering strategy that exploits the unique geometric strength of the Global Positioning System (GPS) to minimize the effects of force model errors has yielded orbit solutions for TOPEX/POSEIDON which appear accurate to better than 3 cm (1σ) in the radial component. Reduction of force model error also reduces the geographic correlation of the orbit error. With a traditional dynamic approach, GPS yields radial orbit accuracies of 4–5 cm, comparable to the accuracy delivered by satellite laser ranging and the Doppler orbitography and radio positioning integrated by satellite (DORIS) tracking system. A portion of the dynamic orbit error is in the Joint Gravity Model-2 (JGM-2); GPS data from TOPEX/POSEIDON can readily reveal that error and have been used to improve the gravity model.

Introduction

In the mid-1980s the TOPEX/POSEIDON project [Fu and Lefebvre, this issue] agreed to develop and fly an experimental Global Positioning System receiver to test the ability of GPS to provide precise orbit determination (POD) by an unconventional new technique [Melbourne *et al.*, 1994]. The GPS receiver aboard TOPEX/POSEIDON tracks the dual L band radio signals from a constellation of 24 GPS satellites, collecting navigation data from up to six satellites at once. Since the orbits and clock offsets of the GPS satellites are known (they are broadcast by the GPS satellites) the receiver can determine its position and time (four unknowns) geometrically at any instant with data from only four satellites. It is this extraordinary geometric strength that distinguishes GPS as a tracking system. Such ground-based systems as SLR (satellite laser ranging) and DORIS (Doppler orbitography and radio positioning integrated by satellite) typically provide measurements in just one direction at a time and may have substantial coverage gaps; they must therefore rely on models of satellite trajectories (derived from models of the forces acting on the satellite) to recover three-dimensional (3-D) information.

With a technique known as reduced dynamic tracking [Wu *et al.*, 1991; Yunck *et al.*, 1990, 1994] we can exploit the 3-D geometric strength of GPS to minimize dependence on dynamic models and, in theory, achieve a superior orbit solution through an optimal synthesis of dynamic and geometric information. A

variation on that technique called kinematic tracking can yield a precise solution almost entirely by geometric means with a sufficiently capable GPS receiver.

Conventional dynamic POD depends on precise models of the forces acting on the satellite to describe the trajectory. In a dynamic solution the estimated parameters will typically include the satellite initial state (position and velocity) and a few quantities describing the force models (e.g., a drag coefficient and once-per-revolution empirical accelerations). These are adjusted to yield a solution that best fits the observations, but that solution will necessarily have errors arising from errors in the force models. With GPS tracking, the model errors can be observed in the 3-D residuals between the orbit solution and the observations. This residual information can then be applied in a point-by-point geometric adjustment of the satellite position to give the reduced dynamic solution (Figure 1). Differences between dynamic and reduced dynamic solutions can expose the model errors and allow us to study their geographical and spectral distribution. Alternatively, parameters describing the gravity field can be adjusted in a dynamic GPS solution to improve (or tune) the gravity model with an unprecedented degree of global strength.

Institutional Roles

This work involved a collaboration between groups at the Jet Propulsion Laboratory (JPL), the Center for Space Research (CSR) of the University of Texas at Austin, and a scientist visiting JPL from the Institut Géographique National (IGN) in Paris. The JPL team focused on refining the reduced dynamic strategy, while CSR, which has long experience in dynamic estimation with SLR, adapted their software for dynamic POD and gravity tuning with GPS data [Rim, 1992]. Although the JPL and CSR analysis systems were developed independently [Wu *et*

Journal of Geophysical Research, 99 (C12):
24,449–24,464 (Dec. 15, 1994).

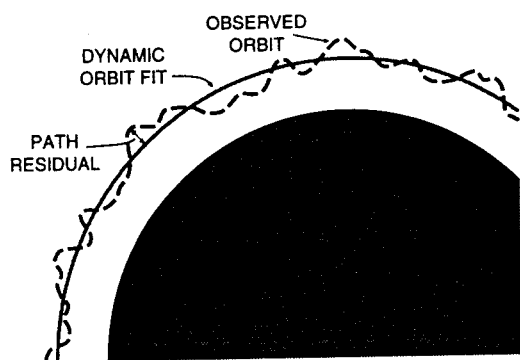


Figure 1. Reduced Dynamic Tracking

al., 1990; Webb and Zumbege, 1993; Rim, 1992], they share some common models. Comparisons between orbits produced with each system serve as an important validation test.

IGN has expertise in the DORIS system and worked closely with JPL to adapt JPL's analysis software to process DORIS data. CSR modified its software independently to process DORIS data as well [Watkins *et al.*, 1992]. In addition, complementary efforts are on-going at the Goddard Space Flight Center (GSFC) and CNES (Centre National d'Etudes Spatiale) in Toulouse to produce the official precise orbits with SLR and DORIS data [Tapley *et al.*, this issue; Nouël *et al.*, this issue].

Experiment Goals

The major goals of the GPS experiment are to (1) evaluate the accuracy and operational potential of GPS for tracking Earth satellites; (2) provide a database that includes the GPS-based orbit solutions, calibration data, and reference frame ties for post experiment use by the project [Born *et al.*, this issue; Christensen *et al.*, this issue]; and (3) provide production GPS POD technology for possible conversion to an operational system.

In the 1980s, covariance analysis suggested that an accuracy of 5 to 10 cm might be achieved if data from six globally distributed GPS ground receivers were used together with the flight data to solve for the TOPEX/POSEIDON orbit [Wu and Ondrasik, 1982; Yunck and Wu, 1986; Wu *et al.*, 1987]. We therefore adopted "better than 10 cm RMS in radial" as a formal goal for the experiment. Analysis further showed that ionospheric calibration with dual frequency GPS data would also be needed. We should note that the flight receiver developed for the experiment can not receive both frequencies when the GPS security feature known as *antispoofing* (AS) is active. It was therefore necessary to arrange with the Department of Defense to have AS off for nine 10-day periods in the first year of the mission to ensure an adequate data set for analysis. Future receiver designs could avoid this problem by adopting either a GPS decryption capability or advanced codeless tracking techniques.

Our objective in evaluating the operational potential of the GPS POD system is to see if GPS can be a cost-effective alternative to existing precise tracking systems. Measures of operational performance include time delay in producing and validating the precise orbit products, reliability of the system, and cost of operation. These operational issues are addressed by Melbourne *et al.* [1993].

Recognizing the potential to support the TOPEX/POSEIDON project more formally, we also set out to (1) collect, edit and archive all data over the experiment lifetime (1 year for the flight

receiver and 2 years for the ground network); (2) tune the gravity model to improve the ocean geoid at wavelengths >1000 km; and (3) make available to the project the most precise orbits for use in oceanographic studies and for altimetric calibration at the verification sites.

System Design

The GPS tracking system consists of four segments: the GPS constellation, the flight receiver, a global network of GPS ground receivers, and a central monitor, control and processing facility (Figure 2). The POD strategy requires continuous tracking of the visible GPS satellites by ground and flight receivers. Data from all receivers are brought together and processed in a grand solution in which the TOPEX/POSEIDON orbit, all GPS orbits, receiver and transmitter clock offsets, carrier phase biases, and a number of other parameters are estimated. Simultaneous sampling at all receivers (which may be achieved by later interpolation) eliminates common errors, such as clock dithering, which is a feature of another GPS security feature known as selective availability (SA). In the end, TOPEX/POSEIDON position and velocity are determined in a reference frame established by key sites in the global network; those sites are known absolutely with respect to the geocenter to 1-2 cm in each component in the International Terrestrial Reference Frame.

The Global Positioning System

Figure 3 depicts the GPS constellation, which is controlled from Falcon Air Force Base near Colorado Springs. The constellation consists of 24 GPS satellites in 12-hr (20,200-km altitude) circular orbits [Milliken and Zoller, 1978; Spilker, 1978]. The satellites are distributed in six orbit planes inclined at 55° , with a nodal separation of 60° . Each satellite broadcasts navigation signals on two L band frequencies: 1.57542 GHz (L1) and 1.2276 GHz (L2). The corresponding carrier wavelengths are approximately 19 and 24 cm. The two frequencies are used to calibrate the ionospheric delay. The beam widths of the GPS signals extend roughly 3000 km beyond the limb of the Earth as

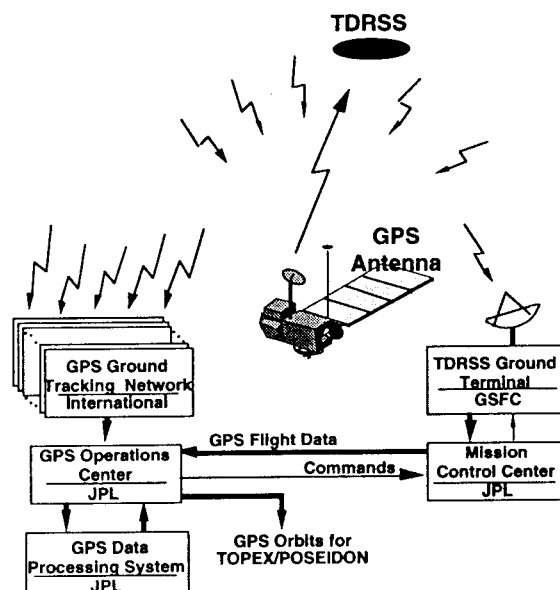


Figure 2. GPS tracking system for TOPEX POD.

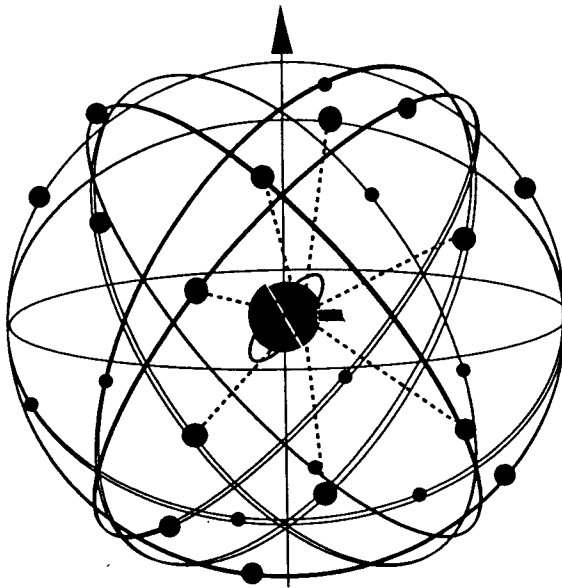


Figure 3. GPS Constellation with TOPEX.

viewed from the GPS satellites. At any point on the Earth's surface, or in the space below 3000 km, typically five to nine GPS satellites are continuously visible within a vertically centered hemispherical field of view. Each *L* band carrier is modulated with a precise pseudo random ranging code known as the *P* code. The receiver measures precisely and unambiguously the arrival time of each code bit; since the transmit time (according to the transmitter clock) of each bit is known, this gives a measure of the pseudorange. Each satellite broadcasts a unique code orthogonal to the others, enabling separation of the received GPS signals. The *L*1 signal is also modulated in quadrature (90° out of phase from the *P* code) by a less precise ranging code known as the coarse/acquisition or *C/A* code. Finally, both *L* band signals are further modulated by a 50 bits/s

data message, which provides accurate GPS orbits, clock offsets from a time standard known as GPS time, satellite health status, and other information of value to the user. For precise applications, dual-band carrier phase measurements, which are recovered by the receiver as part of its code tracking operations, are the primary GPS data type.

Pseudorange is the range between the phase centers of the GPS satellite and receiver antennas, plus the offset between the transmitter and receiver clocks. The pseudorange measurement, however, is corrupted by various other errors. The ground receivers, for example, see an additional delay caused by the Earth's atmosphere. After the ionospheric delay has been removed by dual-frequency combination, carrier phase measures the same quantity as pseudorange, with two distinct differences: it is about 100 times more precise and it has an arbitrary bias resulting from the unknown number of whole cycles between the transmitter and receiver and from various instrumental biases. The ionosphere-free observables are given, in simplified form, by

$$\text{pseudorange} = \text{range} + \text{clock_offset} + \text{troposphere} + \text{noise} \quad (1)$$

$$\begin{aligned} \text{carrier_phase} = & \text{range} + \text{clock_offset} + \text{troposphere} + \text{bias} \\ & + \text{small_noise} \end{aligned} \quad (2)$$

A more detailed description is given by Wu *et al.* [1990].

The GPS Flight Receiver

Figure 4 is a sketch of the TOPEX/POSEIDON spacecraft, showing the locations of some subsystems and flight instruments. The GPS antenna is atop a 4.3-m mast, above the main body of the satellite, to suppress reflected signals from the TDRS high-gain antenna and other prominent surfaces. The GPS Demonstration Receiver (GPSDR), an early version of the Motorola Monarch™ (not visible) tracks up to six GPS satellites concurrently, measuring the phase of each carrier at 1-s intervals and pseudorange at 10-s intervals. Measurement noise on the ionosphere-free observables, including instrumental thermal noise and multipath effects, is about 5 mm for phase and 70 cm for

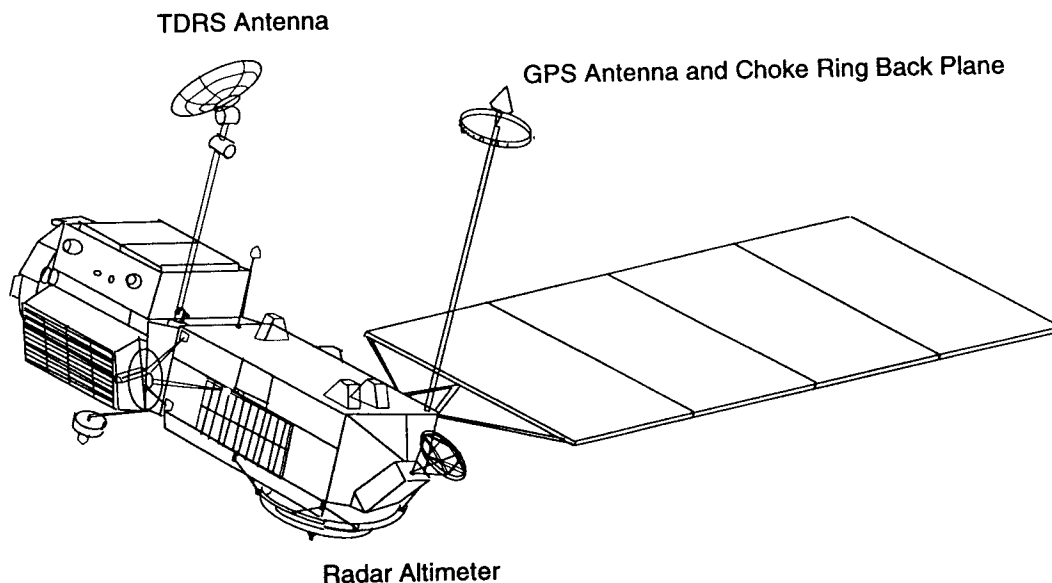


Figure 4. TOPEX/POSEIDON Satellite

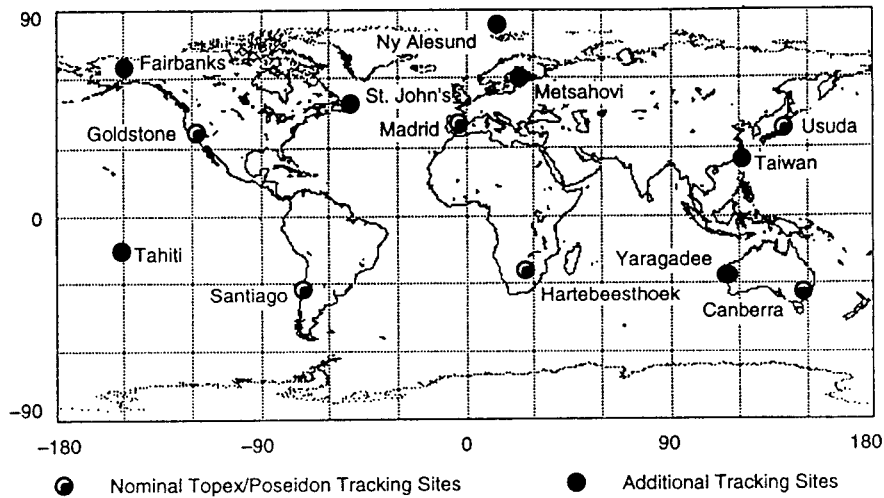


Figure 5. GPS Global Tracking Network

pseudorange. For details on the flight receiver see Zieger *et al.* [1994].

The Global Tracking Network

Figure 5 shows the primary ground sites used in the experiment. These are part of the International GPS Service, which began providing high accuracy GPS data products to scientific users in 1994 under the auspices of the International Association of Geodesy [Neilan and Noll, 1993]. For TOPEX/POSEIDON fewer than a dozen sites are needed to obtain full accuracy because of the ample common GPS visibility between the satellite and the ground sites. For GPS ground programs (which now achieve a weekly geocentric station location precision of about 1 cm), 20-40 sites are sometimes required [Blewitt *et al.*, 1993].

The GPS Operations Center

All transactions involving GPS data and POD products flow through the operations center, which automatically retrieves data from all GPS sources, about 8 Mbyte/d from the flight receiver and 1 Mbyte/d from each ground site. The center monitors and controls the ground and flight receivers and initiates actions to repair system faults. The Rogue™ and TurboRogue™ ground receivers can store their data for, in most cases, up to 12 days to protect against communication outages. In the first 6 months of experimental operations we acquired 99% of the possible data from the flight receiver when GPS anti-spoofing was off, and about 95% from the ground receivers.

Precise GPS-based orbits for TOPEX/POSEIDON are now produced at JPL with 30-hour data arcs on 24-hour centers, providing 6-hour overlaps for comparisons. Those orbits and statistical quality measures are available about 8 hours after all data for a 30-hour arc are received. External release of the orbits occurs about 3 days after the end of each 10-day orbit repeat cycle. Processing of the orbits is automated and data driven. Once the analysis process is initiated on the workstation, it runs continuously, around the clock, with no operator attention except to deal with anomalies. The process wakes up every 3 hours to see if the data for a given arc have arrived. When the required data are there, processing for a 30-hour arc begins.

Solution Strategies

Here we compare TOPEX/POSEIDON precise orbits computed by three groups: JPL, CSR, and GSFC. Each group used different analysis software applied to one or more of three precise tracking data types: GPS, DORIS and SLR. GSFC employs a combination of SLR and DORIS data to deliver operationally the precise orbits placed on the official Geophysical Data Records (GDRs) distributed to scientists [Tapley *et al.*, this issue]. JPL and CSR have performed experimental analysis of the GPS data and have analyzed some combination of SLR and DORIS data as well. While their orbit estimation techniques differ in important ways, the three groups share common models for TOPEX/POSEIDON dynamics and for the positions of observing (or transmitting) points on the Earth relative to inertial space, in which the orbit is propagated. JPL's strategy is unique among the three in its use of Kalman filtering and stochastic models to permit reduced dynamic orbit determination.

TOPEX/POSEIDON Dynamic Models

While the analysis systems share common dynamic models, those models are realized through implementations which give slight differences in the computed ocean tides and earth albedo [Tapley *et al.*, this issue]. All solutions, unless otherwise noted, use the Joint Gravity Model-2 (JGM-2) tuned with TOPEX/POSEIDON SLR and DORIS data [Lerch *et al.*, 1993; Nerem *et al.*, this issue]. A custom model for the solar and thermal radiation forces on TOPEX/POSEIDON was developed for the SLR/DORIS effort [Marshall *et al.*, 1992]. The thermal radiation portion of the model was not used in the JPL GPS solutions, however. These small, slowly varying dynamic model differences can be largely accommodated through the adjustment of an empirical acceleration parameter, \mathbf{a} , of the form

$$\mathbf{a} = \mathbf{C} + \sum_{i=1}^2 \mathbf{A}_i \cos \omega_i t + \mathbf{B}_i \cos \omega_i t \quad (3)$$

where \mathbf{C} , \mathbf{A}_i , and \mathbf{B}_i , are constant vectors in the spacecraft coordinate system oriented in the nominal along-track and cross-track directions [Kaplan, 1976]. The frequencies ω_i are once- and twice-per-revolution of TOPEX/POSEIDON and t is time past an epoch. Solutions produced by CSR (with UTOPIA and

MSODP1) and GSFC (with Geodyn) adjusted constant and once-per-revolution along-track and cross-track amplitudes, while JPL's preliminary dynamic solutions (with GIPSY/OASIS II) adjusted twice-per-revolution terms in those components as well. Empirical once- or twice-per-revolution radial coefficients are not adjusted due to their high correlation with the along-track coefficients.

GPS Dynamic Model

The dynamic model for the GPS satellites contains only two components: the JGM-2 gravity field up to degree and order 12, and custom solar radiation force models known as T10 and T20 [Fliegel *et al.*, 1992].

Earth Models

All three analysis systems use the International Earth Rotation Service (IERS) Standards set forth in IERS Tech Note 13 [McCarthy, 1992; Tapley *et al.*, this issue] for Earth orientation and the deformation of the earth due to solid and pole tides. JPL's GPS solutions estimated polar motion and UT1 with nominal values taken from IERS Bulletin B finals or predicts, depending on the time of processing. The CSR and GSFC solutions employed polar motion and UT1 rate values determined by SLR data from *Lageos* [Tapley *et al.*, this issue].

GIPSY-OASIS II Solution Scenario, Reduced Dynamic Processing

JPL computed dynamic and reduced dynamic solutions with the GIPSY-OASIS II analysis software [Webb and Zumbege, 1993; Wu *et al.*, 1990]. Its main components are a GPS data editor, orbit integrator, measurement model generator, and filter/smoother. The data editor operates on a combined set of dual frequency GPS phase and pseudorange measurements and automatically detects outliers and carrier phase discontinuities [Blewitt, 1990]. An automated executive ties the modules together producing daily orbit solutions unattended. The system typically produces a reduced dynamic solution within 2 days of on-board data acquisition, using less than 6 CPU hours on an HP 735 workstation.

The orbit integrator numerically integrates the satellite trajectory from a nominal initial state using precise models of the forces acting on the satellite. It also computes partial derivatives of the current state of the spacecraft with respect to the dynamical and epoch state parameters. The trajectory and partials are then passed to the measurement model program.

After editing, the data are compressed to 5-min normal points and the ionosphere-free combinations of phase and pseudorange are formed. In the compression step the pseudorange data are smoothed against the carrier over the entire 5-min interval, while the phase is simply sampled at the appropriate times. Because the TOPEX/POSEIDON on-board clock drifts freely with respect to the ground receiver clocks (which are kept close to UTC), we require a small interpolation of on-board phase to the appropriate sample time to ensure common mode cancellation of SA dithering. This is accomplished with a cubic fit to four 1-s points about the desired time [Wu *et al.*, 1992]. The nominal trajectory is then used to compute model GPS observables and their partial derivatives with respect to all adjusted parameters. The measurement model program then retrieves the satellite positions and partials passed by the integrator, computes the model observables, and, in addition, partial derivatives of the observables with respect to ground station position, zenith

troposphere delay, Earth orientation, GPS clocks, and receiver clocks. The observable model includes relativistic effects, the Earth models discussed above, phase windup due to antenna rotation [Wu *et al.*, 1993], and antenna phase center variation as a function of azimuth and elevation [Zieger *et al.*, 1994].

Next the filter/smoother takes over to carry out the grand solution for the TOPEX/POSEIDON and GPS states, ground site positions (five are held fixed for reference), clocks, atmospheric delays, and so on. In its simplest mode, the filter/smoother produces the equivalent of a conventional batch least squares solution; but to obtain a more accurate orbit, some parameters are treated as stochastic processes and adjusted at each time step in a time-sequential square root information filter (SRIF) formulation [Bierman, 1977]. The parameters adjusted in our standard solution strategy are summarized in Table 1.

In these solutions, all clocks are solved for freely and independently at each 5-min time step (i.e., modeled as white noise processes with no a priori constraint), except for one at a ground station which is held fixed as a reference clock. The zenith atmospheric delay at each ground site is also adjusted at each step, modeled as a random walk which in 1 hour adds 1 cm uncertainty in the zenith delay. For the 30-hour data arcs, the parameters of the T10 and T20 solar pressure model [Fliegel *et al.*, 1992] are treated as loosely constrained constants plus a small colored noise process with a 4-hour correlation time and sigma of 10% at 1-hour batch times. The estimation of the GPS orbits is essentially dynamic.

The reduced dynamic solution is produced only in the final estimation step. First, the TOPEX/POSEIDON epoch state and the empirical constant and once- and twice-per-revolution accelerations (Equation 3) are adjusted to convergence in a dynamic solution, which takes two passes through the filter. This dynamic solution is typically accurate to better than 20 cm (3-D), well within the linear regime for the final reduced dynamic adjustment. In the reduced dynamic step, adjustments are made to the TOPEX/POSEIDON state and to all previously adjusted parameters except two types: the empirical once- and twice-per-revolution terms, which are now held fixed, and the constant accelerations (C in equation 3), which now become stochastic and are reestimated at each time step to provide the local geometric corrections. The latter are modeled as first-order Gauss-Markov (colored noise) processes and given a correlation time of 15 min with steady state sigmas of 10, 20, and 20 nm/s² in the radial, cross- and along-track directions. It is the geometric strength of the GPS observations that allows these final stochastic adjustments to be made with high accuracy.

Tuning Stochastic Acceleration Parameters

The steady state sigmas for the stochastic acceleration parameters were chosen through an empirical process in which solutions were generated with a range of sigmas, and the final values selected were those that minimized the RMS differences on the 6-hour orbit overlaps for several test arcs. Once chosen they were held fixed in all processing. A better criterion might be altimeter crossover statistics, but those were not available in our earliest processing and were later reserved as an independent test of orbit accuracy (see tests below).

MSODP1, Gravity Tuning

The Center for Space Research/University of Texas at Austin used MSODP1 (multi-satellite orbit determination program) for the GPS/Topex data processing. The program has been compared

Table 1. Estimation Scenario for Dynamic Filtering of TOPEX/POSEIDON Orbit, GIPSY-OASIS II

Data Type	Data Weight, cm	
Ground carrier phase	1	
Ground pseudorange	100	
T/P carrier phase	2	
T/P pseudorange	300	

Estimated Parameters	Parameterization	A Priori Constraint
T/P epoch state	3-D epoch position	1 km
	3-D epoch velocity	10 cm/s
T/P empirical forces (cross track and along track)	constant	1 mm/s ²
	1- and 2-cycle-per-revolution	1 mm/s ²
T/P antenna phase center offset	radial	5 m
GPS states	3-D epoch position	1 km
	3-D epoch velocity	1 cm/s
GPS Solar Radiation Pressure		
Constant	solar pressure scale factor	100 %
	Y-bias	$2 \times 10^{-3} \mu\text{m/s}^2$
Process Noise (1 hour batch; 4 hour correlation)	X and Z scaling factor	10 %
	Ybias	$10^{-4} \mu\text{m/s}^2$
Nonfiducial station location	ECEF rectangular coordinates	1 km
Tropospheric delay	random-walk zenith delay	50 cm; 0.17 mm/s ^{1/2}
Pole position	X and Y pole	5 m
Pole position rate	X and Y pole rate	1 m/d
UT1 – UTC rate	constant	100 s/d
Carrier phase biases	constant over a continuous pass	3×10^5 km
GPS and receiver clocks	white noise	1 s

All parameters are treated as constants unless otherwise specified

against UTOPIA, the single-satellite orbit determination program used for processing SLR and DORIS data, and the two have agreed at the centimeter level.

MSODP1 uses doubly differenced phase measurements between the flight receiver and the ground stations at 30-s intervals. The higher data rate was used to aid in preprocessing editing and to insure high spatial sampling for gravity field adjustment. For the experiments presented in this paper, double differences between pairs of ground stations were also used for only one cycle specifically for gravity field adjustment. For the other cycles, only double differences involving the flight receiver were used. All double differences were corrected for the ionosphere, and pseudorange measurements were used to compute each receiver clock offset from GPS time.

The MSODP1 uses a batch least squares estimator implemented with a square-root-free Givens algorithm for improved numerical stability. No a priori constraints are assigned to any estimated parameter. A simultaneous solution is performed for the TOPEX/POSEIDON and all GPS satellite states, along with once-per-revolution parameters for TOPEX/POSEIDON and radiation pressure parameters for the GPS satellites. A constant zenith tropospheric delay is estimated at each site every 2.5 hours, and a phase bias parameter is estimated for each combination of TOPEX/POSEIDON, GPS satellite and ground receiver. One-day solution arcs were used in all cases except for the tuning of the gravity field, where 3.3-day arcs were used.

SLR/DORIS Solutions

The precise orbit ephemeris (POE) produced for the altimeter geophysical data records and released to the science community

is computed dynamically by GSFC with SLR/DORIS data over 10-day arcs. They are released only after an extensive validation procedure [Tapley *et al.*, this issue]. We will make comparisons to these official orbits as a test of the GPS reduced dynamic orbits.

Orbit Quality Assessment

First, we describe internal consistency tests within the GIPSY-OASIS II processing system, and then compare the GPS reduced dynamic orbits with the GSFC POE solutions. Next, we present altimetry crossover differences, which provide a test that is independent of all orbit determination techniques and software. Next we examine the difference between the dynamic and reduced dynamic orbits produced with GIPSY-OASIS II to obtain information on the geographically correlated orbit error and its spectral content. The CSR group has recently tuned the JGM-2 gravity model with GPS data; in the final test, dynamic solutions produced by CSR with the tuned field are compared to reduced dynamic solutions made with JGM-2.

Reduced Dynamic Internal Tests

Postfit residuals. As part of the automated quality control, the software examines postfit phase and pseudorange residuals over the full arc. Anomalous data points are automatically detected and removed. Phase residuals for the flight receiver are typically about 5 mm RMS; pseudorange residuals are typically about 70 cm RMS. These values are roughly equal to the combined instrumental noise and multipath error expected on the two observables, implying no substantial mismodeling in the

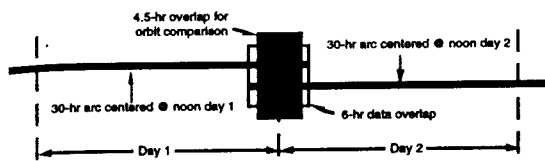


Figure 6. Overlapping data arcs and orbit solutions

estimation process. The GPS data are in general of high quality; only 0.01% of data are detected as anomalous and removed from the filtered solution.

Orbit overlap. TOPEX/POSEIDON data are processed in 30-hour arcs centered on noon UTC (Figure 6). This yields adjacent orbits with 6 hours of overlap. Although the data in the overlap interval are common to the two arcs, the orbit solutions in the overlap are only partially correlated because of the largely independent determination of GPS dynamic orbits and ground station locations for each arc. The orbit overlap agreement is therefore a rough but somewhat optimistic indicator of orbit quality.

To avoid the estimation edge effects (increased error at the ends of the solution arcs resulting from the absence of data on the other side to constrain the stochastic estimate) encountered with reduced dynamic solutions, 45-min segments from each end of the two solutions are omitted in the RMS comparisons. This corresponds to 3 times the time constant used for the stochastic accelerations. A sample of the orbit difference during the central 4.5 hours of the overlap is shown in Figure 7. The RMS difference is 0.88 cm in radial, 5.70 cm cross track and 3.44 cm along track. Figure 8 shows the average RMS overlap agreement in radial for all overlaps for twelve 10-day cycles. The agreement is consistently below 2 cm, with an average of about 1 cm. The anomalous value for cycle 21 appears to have been caused by data outages at Goldstone while Goldstone was used as the reference clock. We have since modified the automated analysis to prevent the use of a reference clock at a station with sizable outages. Cycle 19, which produced the best agreement, was the only cycle in which no GPS satellites passed through the Earth's shadow. During such eclipses the GPS force and measurement model errors increase noticeably. The TOPEX/POSEIDON

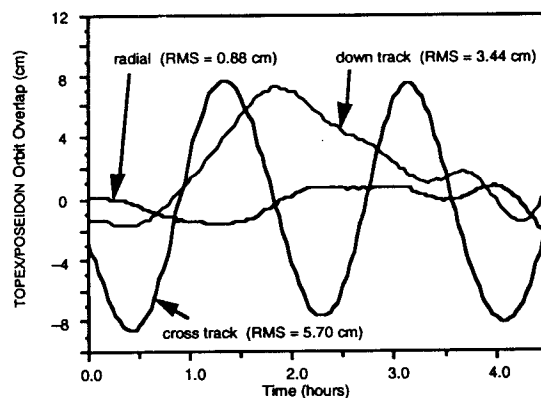


Figure 7. Comparison of overlapping TOPEX/POSEIDON reduced dynamic orbit solutions

dynamic overlap agreement (not shown) is consistently worse, giving single RMS radial overlap differences as high as 5.6 cm and an average RMS difference of about 2 cm.

External Tests

Figures 9 and 10 show the RMS differences between JPL's GPS solutions (both dynamic and reduced dynamic) and the NASA precise orbit ephemeris (POE) over six 10-day repeat cycles. The average RMS radial difference was 2.68 cm for the dynamic comparison and 3.33 cm for the reduced dynamic comparison. The maximum differences in radial position at any point over all six cycles were 12.2 cm (dynamic) and 11.5 cm (reduced dynamic). We shall argue that the better RMS agreement between the two dynamic orbits is the result of common errors in JGM-2 and the non-gravitational force models, errors which are partially removed in the reduced dynamic solution.

In comparing the JPL dynamic and reduced dynamic orbits against the NASA POE, a bias in the mean of the z coordinates of the Greenwich Reference Frame (pseudo-Earth-fixed) of about 3 cm was noticed. This bias varies slightly from cycle to cycle and day to day (Tables 2, 3 and 4). Most of mean differences in the x

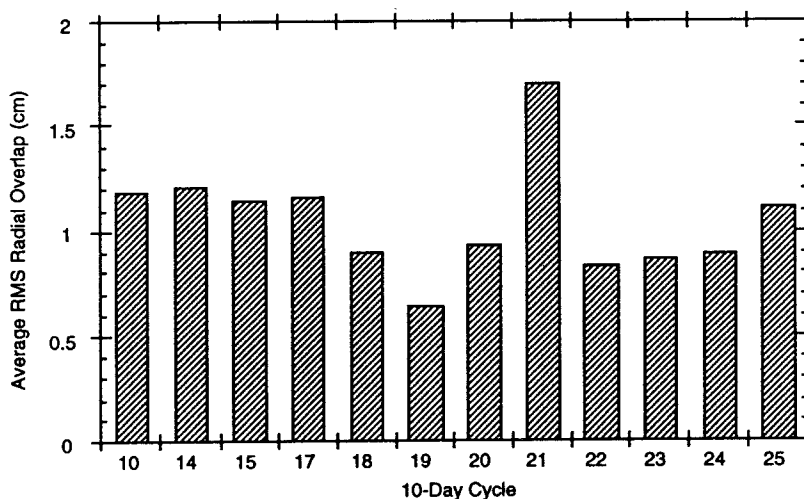


Figure 8. TOPEX/POSEIDON radial reduced dynamic orbit overlaps for twelve complete 10-day cycles

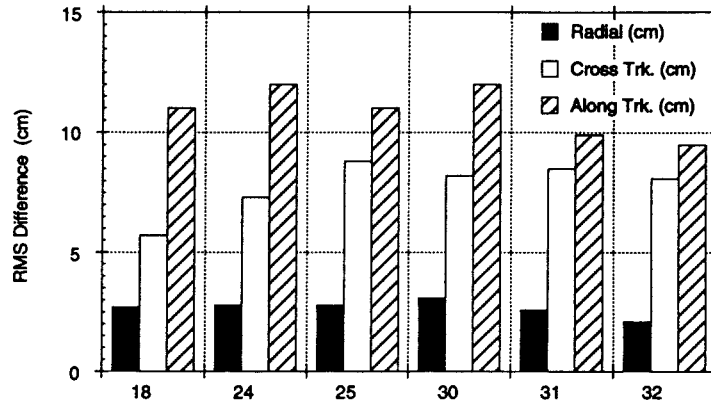


Figure 9. Comparison of TOPEX/POSEIDON dynamic orbit solutions with GPS against Goddard Space Flight Center SLR/DORIS orbits.

and y coordinates can be attributed to errors in JGM-2, as suggested by the much smaller differences in the dynamic solutions (Table 2) and the offset predicted by the difference of dynamic solutions with JGM-2 and JGM-1 [Christensen *et al.*, 1994]. The mean z bias remains essentially unchanged whether a dynamic or reduced dynamic orbit is used in the POE comparison. The z bias also appears in comparisons of the JPL orbits to CSR orbits computed with either GPS or SLR/DORIS data (Table 8). We note that recent determinations of the geocenter from only GPS ground data have obtained decimeter level accuracy in the z component [Vigue *et al.*, 1992]. Inclusion of TOPEX/POSEIDON data in geocenter solutions has improved the observability of this component to about the centimeter level (B. Tapley *et al.*, manuscript in preparation, 1994) and [Malla *et al.*, 1993]. A comparison was also performed with TOPEX/POSEIDON orbits determined by GeoForschungsZentrum (GFZ Potsdam) with GPS data for cycle 15 using a completely independent software system [Kang *et al.*, 1994]. For cycle 15, there was only a 2-mm z bias between JPL reduced dynamic orbits and the GFZ determined orbits while the mean z difference with the NASA POE was 3.5 cm. The RMS radial difference between the NASA POE and the GFZ orbit for

cycle 15 was 3.3 cm. Although the observed z bias between the JPL and other orbits does not appear to reflect a limitation of GPS tracking, we have yet to identify its source and continue to look for it. A 3-cm translation in z reduces the RMS differences by about 3 mm.

If we assume that the errors in the reduced dynamic orbits and the POEs are uncorrelated we can attempt to allocate the 3.33-cm RMS difference. An equal allocation would yield an RMS radial error of 2.35 cm for both solutions. Below, using altimeter crossover analysis and the geographical distribution of errors, we will argue that the errors between the two orbits are largely uncorrelated and that the reduced dynamic orbit error is somewhat smaller.

Altimeter Crossover Analysis

A key method for assessing the relative radial accuracy of different orbits relies on altimeter data collected by the spacecraft. TOPEX/POSEIDON carries two nadir-pointing radar altimeters that measure the range to the sea surface with an uncertainty of less than 4 cm RMS [Fu and Lefebvre, this issue]. These range measurements can be used together with the precise radial orbit solution to determine the geocentric height of the sea

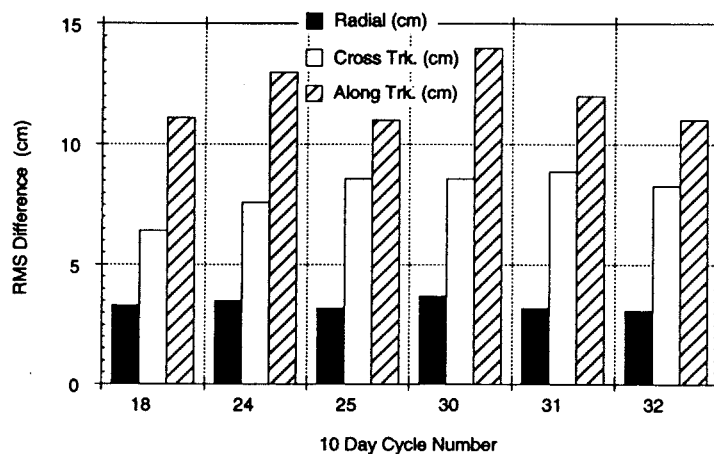


Figure 10. Comparison of TOPEX/POSEIDON reduced dynamic orbit solutions with GPS against Goddard Space Flight Center SLR/DORIS orbits.

Table 2. Mean Coordinate Difference, GSFC POE
— Dynamic

Cycle	X, cm	Y, cm	Z, cm
18	0.06	0.75	2.96
24	0.49	0.11	1.75
25	1.06	0.60	2.66
30	0.21	0.00	3.75
31	0.18	-0.04	3.59
32	0.36	-0.13	1.78

surface. At the points in the ocean where the satellite ground tracks intersect on ascending and descending passes, two such determinations of sea height can be made. In the absence of errors in the radial component of the orbit and in the media corrections to the altimeter range, the height difference at the crossing point location is a measure of the true variability of the ocean surface.

Crossover observations from eight separate 10-day repeat cycles of the TOPEX/POSEIDON ground track were used for this analysis [AVISO, 1993]. Since there is a range bias of about 15 cm between the two altimeter systems [Christensen *et al.*, this issue; Menard *et al.*, this issue], we used only the data from the U.S. dual-frequency altimeter. All standard environmental and sea-state corrections were applied and editing was performed based on the data flags provided with the crossover geophysical records. As crossovers may occur days apart, corrections for ocean dynamic effects, such as those attributable to tides [Cartwright and Ray, 1990] and atmospheric pressure loading, were also applied. A confounding factor is the unmodeled sea height variation from changes in ocean currents and errors in tide models and media corrections. To mitigate the effects of current variations, we restricted our analysis to crossovers occurring within the individual cycles. Table 5 lists the global crossover statistics for the GPS reduced dynamic orbits and for the two precise orbits provided with the merged GDR products. Over 35,000 individual crossovers occurring in the period from January 30 to May 19, 1993, are represented in the global statistic.

The actual radial orbit error is difficult to quantify based on these statistics since the residuals also contain errors in the media corrections and unmodeled oceanographic effects. A large portion of the tidal and atmospheric pressure signal has been removed with global models, but a sizable signal remains. In order to address this difficulty, we have segregated a small number of crossovers from the original global data set using a highly restrictive set of geophysical editing criteria (Table 6). (No outlier editing was performed since it is impossible to guarantee they do not result from large excursions in the orbit error.) These

Table 3. Mean Coordinate Difference, GSFC POE
— Reduced Dynamic

Cycle	X, cm	Y, cm	Z, cm
18	1.23	1.24	2.91
24	2.72	0.72	1.44
25	2.24	0.31	2.24
30	1.70	0.39	3.28
31	1.49	0.49	3.27
32	1.63	1.10	2.21

Table 4 Daily Mean Difference in Z Coordinates,
Cycle 18

	Goddard/JPL Dynamic Z, cm	Goddard/JPL Reduced Dynamic Z, cm
March 10, 1993	3.06	3.51
March 11, 1993	4.45	4.06
March 12, 1993	3.56	2.93
March 13, 1993	2.43	2.28
March 14, 1993	2.50	2.00
March 15, 1993	0.98	0.82
March 16, 1993	5.57	4.99
March 17, 1993	1.31	2.33
Average	2.98	2.86

editing criteria are designed to reduce the ocean variation component of the crossover residuals while maintaining a global distribution of data. To the extent that the geophysical and environmental corrections being interrogated are not correlated with the orbit error, this approach should help to better isolate the orbit error contribution.

Table 7 lists the global crossover statistics for the data remaining after the restrictive editing. Note that while only 3% of the original data remain, there are still over 1000 globally distributed observations (Figure 11). The variance (energy) has been reduced by over 50%, corroborating that the scatter of the original data set primarily reflects contributions from nonorbit sources. Assuming that the residual variabilities are uncorrelated in a global sense on ascending and descending tracks, one could infer that the radial orbit error is less than 5 cm RMS ($7.03/\sqrt{2}$), regardless of the orbit solution under consideration. Contained in this figure is some residual error from the geophysical corrections and instrumental effects, as well as orbit error. On the other hand, if there are large stationary orbit errors that are highly correlated on ascending and descending passes, an extreme example is an error in the overall scale of the orbit, then the crossover observations cannot observe them. Despite these caveats, the crossover statistics provide a powerful and independent tool for measuring orbit consistency and for gauging improvement. In this context, we note that the GPS-based reduced dynamic orbits yield the lowest crossover residuals. In particular, the variances of the crossover populations in both tables (cf. Table 5, Table 7) are about 10 cm² lower with the reduced dynamic orbits, suggesting a consistent reduction in TOPEX/POSEIDON orbit error. If we assume that 3-4 cm of error remains from residual errors in the environmental and geophysical corrections and from ocean variability (a purely speculative number), then we can estimate that the GPS reduced dynamic orbit has a radial RMS error of 2-3 cm while the various dynamic orbits have radial RMS errors of 3-4 cm. The 3-4 cm RMS for dynamic orbit error is consistent with the error estimate of Tapley *et al.* [this issue].

Geographical Error Distribution

Past ocean altimetry missions have been plagued by geographically correlated orbit errors, that is, orbit solutions that are consistently biased in different geographic regions [Rosborough, 1986]. Such errors can confound the interpretation of altimetry data by mimicking large-scale features in the ocean topography from which circulation estimates are derived.

Table 5. Altimeter Crossover Statistics

Orbit	Number	Mean, cm	RMS, cm	Variance, cm ²
GPS reduced dynamic	36403	-0.04	9.69	93.84
NASA precise ephemeris	36403	0.35	10.22	104.41
CNES precise ephemeris	36403	1.04	10.13	101.47

Table 6. Restrictive Editing Criteria for Crossover Evaluation

Parameter	Edit Criteria	Reference
Sea state	Significant wave height < 1 m or > 4 m	AVISO [1993]
Ocean tides	Difference of tide models > 5 cm	Cartwright and Ray [1990], Schwiderski [1980]
Pressure loading	Inverted barometer > 10 cm	AVISO [1993]
Wind speed	Wind speed > 10 m/s	AVISO [1993]
Sea level variability	Mesoscale variability > 12 cm (RMS)	Koblinsky [1990]
Height interpolation	Cubic spline fit RMS > 5 cm	AVISO [1993]

Table 7. Altimeter Crossover Statistics for Restrictive Editing Approach

Orbit	Number	Mean, cm	RMS, cm	Variance, cm ²
GPS reduced dynamic	1233	0.32	6.16	37.85
NASA precise ephemeris	1233	0.68	6.86	46.56
CNES precise ephemeris	1233	1.92	7.03	45.68

Geographically correlated orbit errors are most commonly associated with errors in the gravity model, although coordinate system offsets and other factors may also play a role. A prelaunch covariance study by *Rosborough and Mitchell* [1990] showed that kinematic and reduced dynamic orbits, by reducing dependence on force models in general, could virtually eliminate the geographic correlation in the gravity-induced TOPEX/POSEIDON orbit error at large scales. We have

corroborated this result using the actual GPS-based orbits for TOPEX/POSEIDON.

The differences between GPS-based dynamic and reduced-dynamic TOPEX/POSEIDON orbits over three 10-day periods beginning March 10, March 20, and April 1, 1993, respectively, have been analyzed in terms of the geographical distribution of errors [*Christensen et al.*, 1994]. This analysis suggests that the prelaunch gravity model, JGM-1 [*Nerem et al.*, this issue],

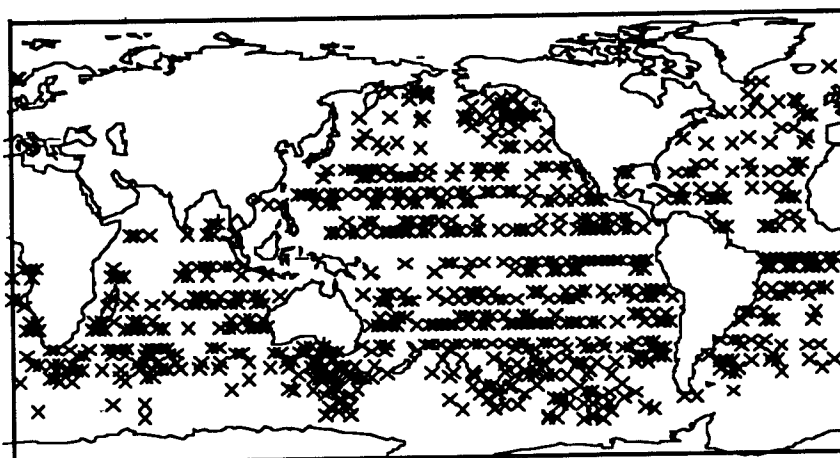


Figure 11. Global distribution of altimeter crossovers used to evaluate orbit accuracy. A stringent editing strategy (Table 6) was applied to crossovers formed from altimeter observations between January 30 and May 19, 1993.

introduces geographically correlated errors having a strong meridional dependence. These errors can be approximated by a large-scale positive anomaly in the Indian Ocean and a large-scale negative anomaly in the eastern Pacific Ocean (cf. of *Christensen et al.*, 1994, Figure 3a). The global distribution and magnitude of these geographically correlated errors are consistent with prelaunch covariance analysis; moreover, the estimated and predicted global RMS error statistics are also in close agreement at 2.3 and 2.4 cm RMS, respectively [*Christensen et al.*, 1994].

Though JGM-2 is a clear improvement over JGM-1, a measurable amount of geographically correlated error, about 1.2 cm RMS according to *Christensen et al.* [1994], persists in the differences between reduced-dynamic and dynamic orbits determined with JGM-2. The salient meridional features are also identified in comparisons between the GPS reduced dynamic orbit and the NASA POE (also based on JGM-2), though the interpretation of this result in the context of gravity error is complicated by ostensible coordinate system differences. Plate 1 shows a 10x10 spherical harmonic expansion of the GPS reduced dynamic and NASA POE differences over a period spanning nearly 250 days. The overall RMS is 2.1 cm; however, some of the energy reflected in this statistic is attributable to the shift between the NASA POE and the GPS-based orbits along the spin axis (discussed elsewhere in this paper.) Removing this shift (2.1 cm) reduces the RMS to 1.8 cm, a number which is in good agreement with the estimate of *Tapley et al.* [this issue] for the mean geographically correlated error present in the NASA POE. Further comparisons between various dynamic and reduced-dynamic orbits should help to separate and identify the sources of

the geographically correlated errors. It should be noted that classical dynamic orbit determination is also capable of observing small modeling errors, such as those introduced by the prelaunch JGM-1 gravity model. To accomplish this, however, the force models must be tuned with comprehensive tracking data from many orbits.

It has long been recognized that differential GPS data can be used with dynamic orbit determination techniques to improve the Earth's gravity model [*Bertiger et al.*, 1992; *Rim*, 1992]. With an improved gravity model, GPS-based dynamic orbits will improve and, for TOPEX/POSEIDON, should approach the accuracy of reduced-dynamic orbits. (Properly weighted, however, the reduced dynamic orbits will in theory remain superior, if only by a small amount, by reducing nongravitational and residual gravity model errors.) For orbiters at much lower altitudes, gravity and aerodynamic forces are extremely difficult to model, and the reduced dynamic technique will be crucial if few-centimeter accuracy is needed.

Spectrum Dynamic Minus Reduced Dynamic Radial

Figure 12 gives the amplitude spectrum of the dynamic-minus-reduced dynamic radial component over 10 days. The spectrum is typical of gravity model error in a dynamic solution, which, because of the daily rotation of the field, generates a suite of tones at $1/\text{revolution} \pm m/d$ [*Rosborough*, 1986]. The $\pm m/d$ tones in the spectrum may also include artifacts from the daily orbit fits spliced together to form a 10-day solution. Notice that nearly all of the energy is at frequencies below twice/revolution.

See original source for Plate 1
(Color Original)

Plate 1. Geographic representation of orbit height differences for NASA POE (JGM-2) and GPS reduced-dynamic orbits. A 10x10 spherical harmonic fit to the data captures a signal with rms amplitude of 2.1 cm.

Table 10. Changes From Table 9 for Earth Observing System Kinematic Orbit Determination Analysis

Parameter	Description
Orbit (circular)	705 km, 98° inclination
Number of GPS satellites	24
Flight receiver tracking	All in view capacity (within hemisphere)
Zenith atmospheric delay error	Adjusted as random walk
Fiducial location error	3 cm each component
Earth gravity error model	100% GEM10-GEML2 (20x20)

nominal location as specified on the drawings to within 2 mm in the z component and within 8 mm three dimensional. An anomaly exists somewhere in the overall model of the GPS observable. Although an error in the satellite measurements would explain the results, we have all but ruled that out based on other evidence and as yet have no satisfactory explanation for the apparent antenna bias. There is a slim possibility that the offset could result from incomplete knowledge of the phase center of the GPS transmitters. A preliminary analysis, however, shows extremely small variation of the GPS satellite phase center with look angle. Meanwhile, we continue to estimate a phase center offset, even though it is now well characterized.

Implications for the Future

Results from this experiment confirm the accuracy of prelaunch GPS error studies and lend confidence to predictions made by similar studies for future missions. Figure 15 summarizes a TOPEX/POSEIDON study, performed several years before launch, in which the gravity field error is modeled as a percent of the difference between the models GEM10 and GEML2 [Wu *et al.*, 1991]. The assumptions (Table 9) were in many ways inconsistent with what has been done in the actual 30-hour JPL solutions. The available computing power at the time was meager by today's standards, necessitating the use of shorter data arcs.

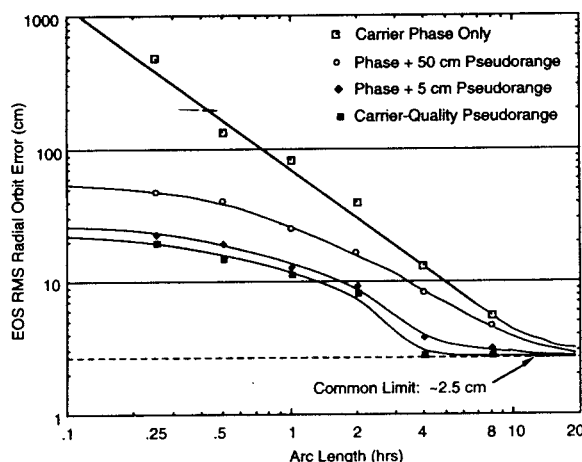


Figure 16. Covariance analysis prediction for future a 700 km radial mission.

Table 11. Changes From Table 9 for Shuttle Kinematic Orbit Determination Analysis

Parameters	Description
Orbit (circular)	300 km, 28° inclination
Number of GPS satellites	24
Number of ground sites	11 (including 3 fiducial sites)
Flight antenna field of view	Full sky
Flight receiver tracking capacity	All in view
Smoothed data noise	5 cm pseudorange, 5 mm carrier phase
Zenith atmospheric delay error	Adjusted as random walk
Fiducial location error	1.5 cm each component
Earth gravity error model	50% GEM10-GEML2 (20x20)

To compensate, we assumed a 2-m a priori error on the GPS orbits and a low pseudorange noise of 5 cm. The estimated 2–3 cm RMS radial error for the reduced dynamic solution with JGM-2 is plotted (point x) in Figure 15 along with the typical observed RMS difference between reduced dynamic and SLR/DORIS solutions (point a). The position of GEM-T1 on the x axis was determined by a consider analysis using the full GEM-T1 covariance matrix. The position of JGM-2 on the x axis relative to GEM-T1 was determined by comparing the radial errors predicted by perturbation analyses using the associated covariance matrices for JGM-2 and GEM-T1 [Rosborough, 1986; Nerem *et al.*, this issue]. Somewhat fortuitously, the artificial compensation has proved reasonably accurate, and the agreement with the estimated actual error is within a centimeter.

One future mission we have studied is the Earth Observing System, a suite of scientific Earth probes planned to fly at about 700 km beginning in the late 1990s. Because dynamic model error can grow large at that altitude, a purely kinematic analysis is presented. The reference site error is now reduced to 3 cm per component and the number of flight receiver channels is increased to track all satellites within a hemisphere, which increases the geometric strength compared to TOPEX/POSEIDON. Other assumptions that differ from the TOPEX/POSEIDON covariance analysis are given in Table 10. Figure 16 shows the predicted radial error as a function of data arc length for several different GPS data combinations. The data type called "carrier-quality range" is a fictitious pseudorange measurement having the precision of carrier phase, and serves to establish a performance bound. With data arcs longer than 20 hours, all scenarios yield about 2.5 cm RMS radial errors for kinematic tracking, which is virtually independent of dynamic model error.

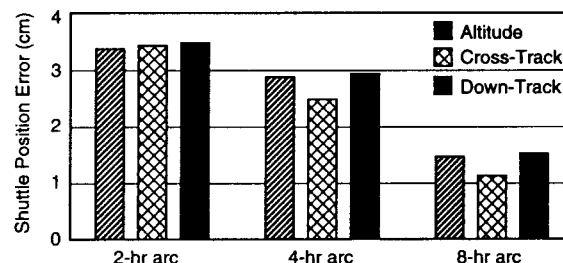


Figure 17. Predicted error for the Space Shuttle viewing all possible GPS within a sphere

To see what might be done with even greater geometric strength we present a study of the Space Shuttle at 300 km, in which we open up the flight receiver field of view to the full sky (each shuttle is equipped with GPS antennas top and bottom to permit this). Typically, there will be 13–15 GPS satellites in view at once. Other assumptions are given in Table 11. As shown in Figure 17, the limiting error in all components now falls below 2 cm. This opens up new possibilities for near-Earth ocean altimetry, and for short-duration testing of precise instruments on the shuttle. We should note, however, that covariance analysis can be optimistic, particularly for kinematic estimation, and unmodeled systematic errors could at least double the actual error in these examples.

Conclusions

The evidence suggests that we are obtaining a radial orbit accuracy for TOPEX/POSEIDON of better than 3 cm RMS with the GPS reduced dynamic technique. Tests of orbit quality include postfit phase residuals (~5 mm), orbit overlap comparisons (~1 cm radial RMS), comparison with GSFC POEs (3.3 cm radial RMS; 11.5 cm maximum difference for 6 cycles), and altimeter crossovers (9 cm² smaller variance than the NASA POE or CNES orbits). The reduced dynamic orbits substantially reduce the geographically correlated error arising from the gravity model. Tuning of the gravity model with GPS data has resulted in a similar reduction of geographically correlated error in subsequent dynamic orbit solutions with all data types. Future missions can take advantage of the operational GPS system developed for this experiment and should obtain radial RMS accuracies of 5 cm or better in orbits as low as a few hundred kilometers.

Acknowledgments. The work described in this paper was carried out in part by the Jet Propulsion Laboratory, California Institute of Technology, under contract with the National Aeronautics and Space Administration. We thank Steve Nerem of Goddard Space Flight Center, John Ries of the Center for Space Research at the University of Texas at Austin, and George Rosborough of the University of Colorado for their help and comments. The GPS Network Operations Group at JPL provided automated access to the data from the GPS ground network (sponsored by NASA's Office of Space Communications). The TOPEX/POSEIDON POD Team chaired by Byron Tapley of the University of Texas, and including members from GSFC, CCAR, and CSR, provided valuable information on modeling TOPEX/POSEIDON and did much to stimulate this work. The computer systems and network support of Mike Urban and Michael Kelsay contributed to the JPL systems ease of use. The Satellite Geodesy and Geodynamics Systems Group at JPL helped develop GIPSY-OASIS II and made valuable contributions to this work.

References

- AVISO, Aviso User Handbook: Merged TOPEX/POSEIDON products, Rep. AVI-NT-02-100-CN, 2nd ed., CNES, Toulouse, France, 1993.
- Bertiger, W. I., J. T. Wu, and S. C. Wu, Gravity field improvement using GPS data from TOPEX/POSEIDON: a covariance analysis, *J. Geophys. Res.*, 97, 1965-1971, 1992.
- Bierman, G. J., *Factorization Methods for Discrete Sequential Estimation*, Academic, San Diego, CA, 1977.
- Blewitt, G., An automatic editing algorithm for GPS data, *Geophys. Res. Lett.*, 17(3), 199-202, 1990.
- Blewitt, G., M. B. Heflin, K. J. Hurst, D. C. Jefferson, F. H. Webb, and J. F. Zumberge, Absolute far-field displacements from the 28 June 1992 Landers earthquake sequence, *Nature*, 361, 340-342, 1993.
- Born, G., M. Parke, P. Axelrad, K. Gold, J. Johnson, K. Key, D. Kubitschek, and E. Christensen, Calibration of the TOPEX altimeter using a GPS buoy, *J. Geophys. Res.*, this issue.
- Cartwright, D. E., and R. D. Ray, Ocean tides from Geosat altimetry, *J. Geophys. Res.*, 95, 3069-3090, 1990.
- Christensen, E. J., C. S. Morris, B. J. Williams, J. R. Guinn, B. J. Haines, C. K. McColl, R. A. Norman, S. J. Keiham, D. A. Imel, and G. H. Born, Calibration of TOPEX/POSEIDON at Platform Harvest, *J. Geophys. Res.*, this issue.
- Christensen, E. J., B. J. Haines, K. C. McColl, and R. S. Nerem, Observations of geographically correlated orbit errors for Topex/Poseidon using the Global Positioning System, *Geophys. Res. Lett.*, 21(19), 2175-2178, 1994.
- Fliegel, H. F., T. E. Gallini, and E. R. Swift, Global Positioning System radiation force models for geodetic applications, *J. Geophys. Res.*, 97, 559-568, 1992.
- Fu, L. L., M. Lefebvre, E. Christensen, C. Yamerone Jr., Y. Menard, M. Dorner, and P. Escudier, TOPEX/POSEIDON mission overview, *J. Geophys. Res.*, this issue.
- Kang, Z., P. Schwintzer, C. Reigber, and S. Y. Zhu, TOPEX precise orbit determination and gravity field improvement using GPS-SST, A. G. 12, suppl., in press, 1994.
- Kaplan, M. H., *Modern Spacecraft Dynamics and Control*, John Wiley, New York, 1976.
- Koblinsky, C. J., Geosat vs Seasat, *Eos Trans. AGU*, 69(44), 1026, 1990.
- Lerch, F., et al., Gravity model improvement for TOPEX/POSEIDON, *Eos Trans. AGU*, 74(16), 96, 1993, (abstract), Spring Meeting, suppl.
- Malla, R. P., S. C. Wu, S. M. Lichten, and Y. Vigue, Breaking the ΔZ barrier in geocenter estimation, *Eos Trans. AGU*, 74(43), 182, 1993(abstract), Fall Meeting, suppl.
- Marshall, J. A., S. B. Luthcke, P. G. Antreasian, and G. W. Rosborough, Modeling radiation forces acting on TOPEX/POSEIDON for precision orbit determination, *NASA Tech. Memo. 104564*, 1992.
- McCarthy, D. D. (Ed.), *IERS Tech. Note 13*, C. B. of Int. Earth Rotation Serv., Obs. de Paris, France, July 1992.
- Melbourne, W. G., E. S. Davis, T. P. Yunck, and B. D. Tapley, The GPS Flight Experiment on TOPEX/POSEIDON, *Geophys. Res. Lett.*, 21(19), 2171-2174, 1994.
- Melbourne, W. G., T. P. Yunck, W. I. Bertiger, B. J. Haines, and E. S. Davis, Scientific applications of GPS on low Earth orbiters, *J. Satell. Based Positioning Navig. Commun.* 119-145, 1993.
- Menard, Y., E. Jeansou, and P. Vincent, Calibration of the TOPEX/POSEIDON altimeter over Lampedusa: Additional results at Harvest, *J. Geophys. Res.*, this issue.
- Milliken, R. J., and C. J. Zoller, Principle of operation of NAVSTAR and system characteristics, *Navigation*, 25, 95-106, 1978.
- Neilan, R. E., and C. E. Noll, The IGS core and fiducial networks: current status and future plans, in *Proceedings of 1993 IGS Workshop*, Astronomical Institute, University of Bern, Switzerland, 1993.
- Nerem, R. S., et al., Gravity model development for TOPEX/POSEIDON: Joint gravity models 1 and 2, *J. Geophys. Res.*, this issue.
- Nouël, F., J. P. Berthias, M. Deleuze, A. Guitart, P. Laudet, A. Piuze, D. Pradines, C. Valorge, C. Dejoie, M. F. Susini, and D. Taburiau, Precise Centre National d'Etudes des Telecommunications, orbits for TOPEX/POSEIDON: is reaching 2 cm still a challenge?, *J. Geophys. Res.*, this issue.
- Rim, H., TOPEX orbit determination using GPS tracking system, Ph.D. dissertation, Univ. of Tex. at Austin, 1992.
- Rosborough, G. W., Satellite orbit perturbations due to the geopotential, Ph.D. thesis, 155 pp., Univ. of Tex. at Austin, 1986.
- Rosborough, G., and S. Mitchell, Geographically correlated orbit error for the TOPEX satellite using GPS tracking, paper presented at AIAA/AAS Astrodynamics Conference, Part 2, Am. Inst. of Aeron. and Astron., Portland, Oregon, Aug. 1990.
- Schutz, B. E., B. D. Tapley, P. A. M. Abusali, and H. J. Rim, Dynamic orbit determination using GPS measurements from TOPEX/POSEIDON, *Geophys. Res. Lett.*, 21(19), 2179-2182, 1994.
- Schwiderski, E. W., On charting global ocean tides, *Rev. Geophys.*, 18, 243-268, 1980.

- Spilker, J. J., GPS signal structure and performance characteristics, *Navigation*, 25, 29-54, 1978.
- Tapley, B., et al., Precision orbit determination for TOPEX/POSEIDON, *J. Geophys. Res.*, this issue.
- Vigue, Y., G. Blewitt, S. M. Lichten, M. B. Heflin, and R. J. Muellerschoen, Recent high-accuracy GPS estimates of the geocenter(abstract), *Eos Trans., AGU*, 73 (43), Fall Meeting suppl. 135, 1992.
- Watkins, M. M., J. C. Ries, and G. W. Davis, Absolute positioning using DORIS tracking of the SPOT 2 satellite, *Geophys. Res. Lett.*, 19(20), 2039-2042, 1992.
- Webb, F. H., and J. F. Zumberge (Eds.), *An Introduction to GIPSY/OASIS II*, JPL Document D-11088, Jet Propuls. Lab., Pasadena, Calif., July, 1993.
- Wu, J. T., S. C. Wu, G. H. Hajj and W. I. Bertiger, Effects of antenna orientation on GPS carrier phase, *Manuscr. Geod.*, 18(2), 91-98, 1993.
- Wu, S. C., and V. J. Ondrasik, Orbit determination of low-radial Earth satellites using GPS RF Doppler, in *Proc. IEEE Position Location and Navigation Symp.*, pp 85-91, 1982.
- Wu, S. C., Y. Bar-Sever, S. Bassiri, W. I. Bertiger, G. A. Hajj, S. M. Lichten, R. P. Malla, B. K. Trinkle and J. T. Wu, TOPEX/POSEIDON Project: Global Positioning System (GPS) Precision Orbit Determination (POD) Software Design, *Rep. JPL D-7275*, Jet Propuls. Lab., Pasadena, Calif., March 1990.
- Wu, S. C., T. P. Yunck, and C. L. Thornton, Reduced-dynamic technique for precise orbit determination of low Earth, *J. Guid., Control Dyn.*, 14(1), 24-30, 1991.
- Wu, S. C., W. I. Bertiger, and J. T. Wu, Minimizing selective availability error on TOPEX GPS measurements, *J. Guid., Control Dyn.*, 15(5), 1306-1309, 1992.
- Yunck, T. P. and S. C. Wu, Non-dynamic decimeter tracking of Earth satellites using the Global Positioning System, presented at AIAA 24th Aerospace Sciences Meeting, Am. Inst. of Aeron. and Astron., Reno, Nev., Jan. 1986.
- Yunck, T. P., S. C. Wu, J. T. Wu, C. L. Thornton, Precise tracking of remote sensing satellites with the Global Positioning System, *IEEE Trans Geosci Rem Sens* (28), Jan 1990.
- Yunck, T. P., W. I. Bertiger, S. C. Wu, Y. Bar-Sever, E. J. Christensen, B. J. Haines, S. M. Lichten, R. J. Muellerschoen, Y. Vigue, and P. Willis, First assessment of GPS-based reduced dynamic orbit determination on TOPEX/POSEIDON, *Geophys. Res. Lett.*, 21, 541-544, 1994.
- Zieger, A. R., G. C. Cleven, E. S. Davis, F. S. Soltis, and C. L. Purdy, Satellite/sensors for monitoring Earth's oceans from space, *Mar. Geod.*, in press, 1994.
- W. I. Bertiger, Y. E. Bar-Sever, E. J. Christensen, E. S. Davis, J. R. Guinn, B. J. Haines, R. W. Ibanez-Meier, J. R. Jee, S. M. Lichten, W. G. Melbourne, R. J. Muellerschoen, T. N. Munson, Y. Vigue, S. C. Wu, and T. P. Yunck, 48000 Oak Grove Drive, Jet Propulsion Laboratory, California Institute of Technology, Pasadena, CA 91109-8099. (e-mail: wib@cobra.jpl.nasa.gov)
- B. E. Schutz, P. A. M. Abusali, H. J. Rim, and M. M. Watkins, Bureau of Engineering Research, University of Texas Center for Space Research/WRW 402, Austin TX 78712. (e-mail: schutz@utcsr.ac.utexas.edu)
- P. Willis, Institut Géographique National, 2 Avenue Pasteur, BP 68, 94160 Saint-Mande, France (e-mail: willis@schubert.ign.fr).

(Received November 19, 1993; revised May 2, 1994;
accepted May 2, 1994.)